Communication

Poynting Streamlines, Effective Area Shape, and the Design of Superdirective Antennas

Junming Diao and Karl F. Warnick

***Abstract*— A receiving antenna alters an incident field in such a way that the field is concentrated at the terminals of the antenna. The Poynting power flux density vector associated with the field carries to the antenna the power dissipated in the antenna structure and the load. Streamlines of the Poynting vector field can be used to understand electromagnetic energy flow near linear and aperture antennas. Poynting streamlines provide a way to understand and guide the design of superdirective antennas. Directivity-enhancing screens that attract Poynting streamlines and increase the aperture efficiency of a horn antenna to almost 200% are studied. Superdirective antennas generally have limited practical value due to poor radiation efficiency, narrow bandwidth, and extreme sensitivity to fabrication errors. We show that these limitations can be mitigated by using metal-only structures that are optimized for broadband operation. The tradeoff between peak achievable aperture efficiency and bandwidth is explored.**

***Index Terms*— Effective area shape, Poynting streamlines, receiving antenna, superdirective antenna.**

I. Introduction

Antennas are commonly modeled and understood as transmitters, and reciprocity is used to obtain the receiving properties of the antennas. While it is less common in the field of antenna theory, antennas can also be analyzed directly as receivers. A receiving antenna can be viewed as a field concentrating device. The electric field associated with an incident wave is influenced by the presence of the antenna structure in such a way that fields near the antenna are bent and concentrated, so that a high electric field appears at the antenna terminals and power is delivered to the antenna load. The energy flow distribution near the antennas and the effective area shapes can be calculated using streamlines of the Poynting vector field. The existence of streamlines, integral curves, or flow lines for vector fields is a topic of differential geometry [1]. Physically, streamlines, which terminate on the antenna load, correspond to power absorbed by the antenna, and streamlines that miss the antenna represent power that is not absorbed. The locus of streamlines that terminate on the antenna load provides a way to assign a geometrical shape to the effective area [2].

The Poynting streamline method has been used by several authors to analyze wire antennas [2]–[4]. We have extended the Poynting streamline method to aperture antennas and guide the design of superdirective antennas. Using the finite-element method and post-processing to compute streamlines of the Poynting vector field, we use Poynting streamlines to study the effect of the antenna on the power flow in the electromagnetic field near dipoles, conventional horns, and superdirective horn antennas. The Poynting streamline approach is used to assign a geometrical shape to the effective area of these antennas, and we find that this shape reflects the physical behavior of the antenna in interesting ways.

For superdirective antennas, Poynting streamlines over a larger area than the aperture are attracted to the antenna and terminated on the load. For an arbitrary aperture field distribution, there is no limit on directivity, and Poynting streamlines over an arbitrarily wide area can be attracted to the antenna. Practical considerations, however, limit both the degree of achievable superdirectivity and the usefulness of superdirective antennas. Drawbacks include narrow bandwidth, low radiation efficiency, and extreme sensitivity to perturbations and fabrication errors [5]. Due to ohmic or dielectric losses exacerbated by intense near fields and currents on the antenna structure, radiation efficiency can be poor for superdirective antennas, meaning that superdirectivity does not necessarily imply that the antenna achieves a higher gain than a uniformly illuminated aperture antenna of the same size.

Superdirectivity is typically implemented for small antennas by extending the near field distribution of the antenna in a variety of ways. Less attention has been given to superdirectivity for electrically large antennas. High-directivity horn antennas have been designed using corrugated structures [6], dielectric lenses [7], and metamaterials [8]. We use the Poynting streamline method to enhance the gain of a traditional TE_{10} horn antenna. The horn antenna with gain enhanced by a screen of rods achieves a modeled aperture efficiency from 80% to almost 200%. We also give a design that achieves broadband operation, overcoming a practical limitation of most narrowband superdirective antennas.

Two different metal screen structures for the superdirective horn antenna are compared over frequency; the relationship between the bandwidth and superdirectivity is studied, and the impact of loss on radiation efficiency is considered over the superdirective operating regime. Through these examples, Poynting streamlines are shown to be a useful tool in understanding the physics of receiving antennas and in creating superdirective antennas that promise better performance than has been realized in the past.

II. Numerical Analysis

A full-wave numerical model is used to study Poynting streamlines for receiving antennas. In order to focus on the field bending effect influenced by the directivity and antenna structure, the antenna load is conjugate matched to the antenna input impedance and the antenna structure is assumed to be lossless except where otherwise indicated.

The Poynting vector associated with the total field is computed from the electric and magnetic field for a uniform plane wave normally incident on the antenna [4]. The antenna polarization is assumed to be aligned with the incident field. For convenience in software implementation, we extract the Poynting vector on a cut plane that passes through the phase center of the antenna. Streamlines are generated in postprocessing for each cut plane by

Manuscript received January 26, 2016; revised June 13, 2016 and September 21, 2016; accepted September 25, 2016. Date of publication November 23, 2016; date of current version February 1, 2017.

The authors are with the Department of Electrical and Computer Engineering, Brigham Young University, Provo, UT 84602 USA (e-mail: diaojunming@gmail.com; warnick@ee.byu.edu).

Color versions of one or more of the figures in this communication are available online at http://ieeexplore.ieee.org.

Digital Object Identifier 10.1109/TAP.2016.2632618

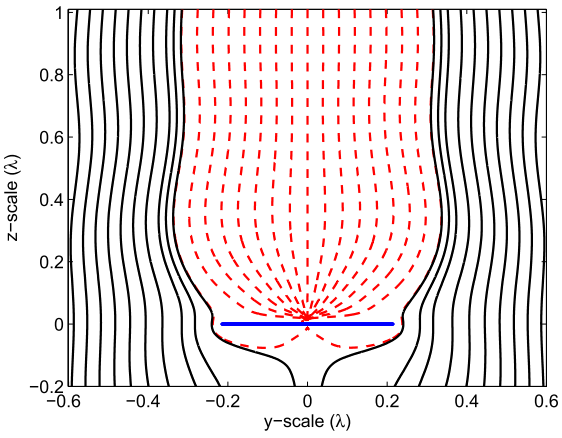

(a)

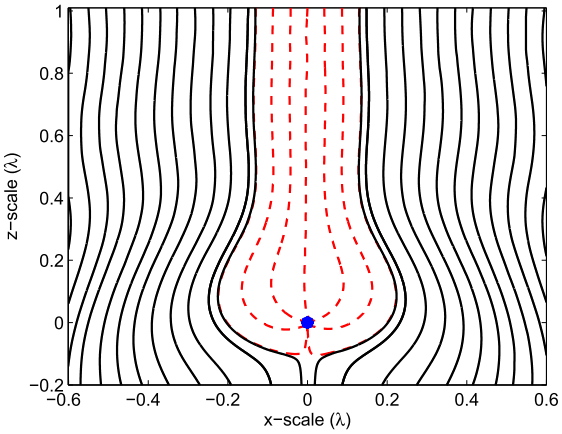

(b)

Fig. 1. Streamline for the Poynting vector of the total fields for a simple dipole antenna with 0.43λ length. The horizontal straight line represents the actual size of the dipole antenna. (a) E-plane. (b) H-plane.

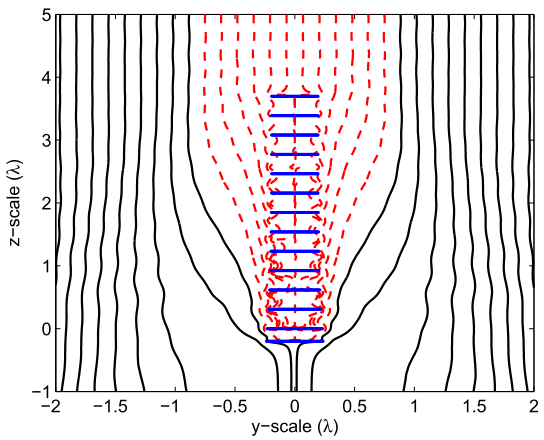

(a)

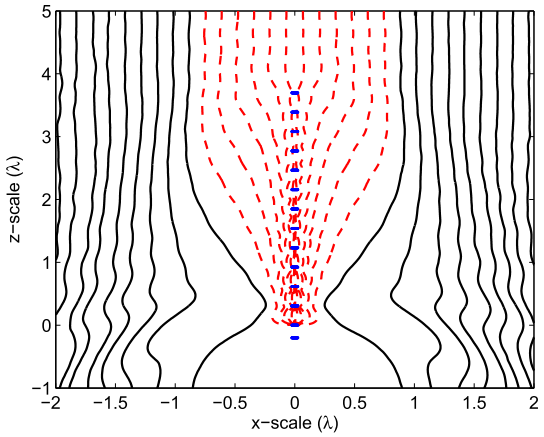

(b)

Fig. 2. Streamlines for the Poynting vector of the total fields for a 15-element Yagi–Uda antenna. The excitation element length is 0.47λ. (a) E-plane. (b) H-plane.

finding paths that are everywhere tangential to the Poynting vector field.

A. Wire Antennas

As an illustration of the Poynting streamlines technique, we consider a dipole antenna and a 15-element Yagi–Uda antenna. For the dipole antenna, the length and the diameter are 0.43λ and 0.017λ, respectively. A lumped port load is used between two dipole arms with a feed gap of 0.017λ. For the Yagi–Uda antenna, the antenna axial length and the driven elements length are 3.9λ and 0.47λ, respectively. The parameters for the reflector and driven element are given in [9]. The loads for both antennas are conjugate matched to the antenna input impedance and the antenna S_{11} relative to a 50-Ω system impedance is -15.6 and -10 dB, respectively. A uniform plane wave is incident on the antennas from the broadside direction.

The resulting streamline distributions for the dipole and Yagi–Uda antennas are shown in Figs. 1 and 2. Streamlines terminated by the antenna load are marked with dashed color, and the nonabsorbed streamlines are marked with solid line. The physical profile of the antennas is marked with straight solid line. In the E-plane, the Poynting streamlines are concentrated along the top of the dipole arm in the direction of the antenna load. Compared with the E-plane, fewer streamlines in the H-plane are terminated by the antenna load, which reflects the broader radiation pattern in the H-plane. For the Yagi–Uda antenna, streamlines are concentrated along the director elements and then transmitted to the driven element.

Poynting streamlines that are absorbed by the antenna load are associated with the shadow of the antenna as reflected by a decrease in the total field beyond the antenna relative to the arrival direction of the incident field. Near the antenna, due to the scattering from the antenna structure, some of the Poynting streamlines deviate from the straight paths associated with the incident field, but are not absorbed by the antenna load.

The IEEE standard definition of effective area is given by [10]

$$A_e = \frac{P_T}{W_i} \tag{1}$$

where P_T is the available power at the terminals of a receiving antenna and W_i is the power flux density of a plane wave incident on the antenna from that direction with the aligned polarization to the antenna. The effective area definition provides only the scalar magnitude of this antenna parameter, and yields no information about the shape of an antenna's receiving area. For the dipole example, the receiving area can be assigned a geometrical shape using the Poynting streamline method.

For the dipole example, the Poynting streamlines terminated by the dipole antenna load extend from $(0, -0.31)$ to $(0, 0.31)$ in the E-plane. The terminated boundary of Poynting streamlines in each cut plane spans a 2-D locus that provides a geometrical shape for the effective area of the antenna. Fig. 3 shows the load terminated

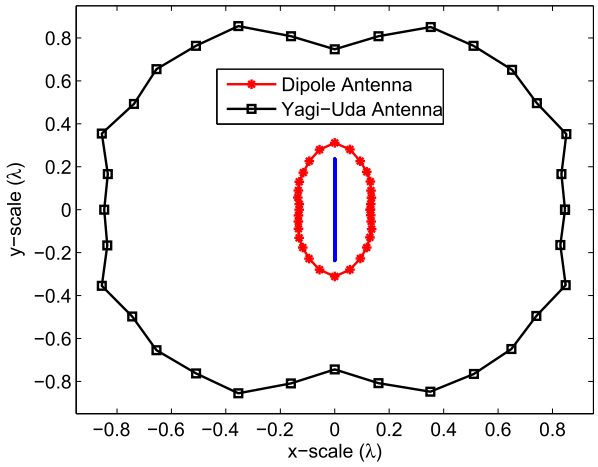

Fig. 3. Comparison of Poynting streamline area shapes for a dipole and 15-element Yagi–Uda antenna.

TABLE I
ACCURACY ANALYSIS

Antenna Type	A_e (λ^2)	A_s (λ^2)	Difference
Dipole	0.126	0.133	5.2%
Yagi-Uda	2.633	2.579	2.1%
Traditional Horn	0.898	0.961	6.6%
Superdirective Horn	2.128	1.997	6.3%

Poynting streamline area shape for the dipole and Yagi–Uda antenna. It can seen that the shape of the locus of terminated streamlines is consistent with the analysis of [3], and the area of the locus is close to the effective area of the antenna calculated from its directivity. A comparison of the Poynting streamline area and the effective area is given in Table I.

The Poynting streamline area shape of the Yagi–Uda antenna is close to circular. Normally, a high-gain antenna is designed by maximizing gain, which is equivalent to maximizing the effective area. This suggests that antenna designs that achieve a circular or near circular Poynting streamline area are more effective than designs with elongated streamline areas, as they better utilize the space around the antenna to capture power in the incident wave.

B. Traditional TE_{10}*-Mode Horn Antenna*

We now extend the Poynting streamline method to an aperture-type horn antenna. In Fig. 4, Poynting streamlines for a $0.75\lambda \times 1.5\lambda$ horn antenna with TE_{10}-mode aperture field distribution are shown. Compared with the H-plane, more streamlines are terminated by the antenna load in the E-plane, which is consistent with the narrower beamwidth in the H-plane.

Fig. 5 shows the Poynting streamline area shape and the induced aperture field distribution of the horn antenna corresponding to a normally incident plane wave. The Poynting streamline area shape and the aperture field distribution are close to the TE_{20}-mode field distribution, which is reasonable, since the width of horn antenna is larger than the cutoff wavelength of the TE_{20}-mode. For the same horn operated as a transmitter, the aperture field behaves as a TE_{10}-mode distribution, which is different from the field in receive mode. This might seem surprising, as it appears to violate the reciprocity theorem, but reciprocity actually still holds, and the receiving and transmitting properties of the antenna are related in the usual way.

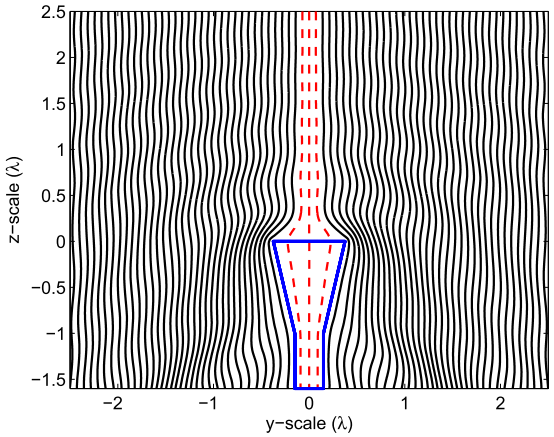

(a)

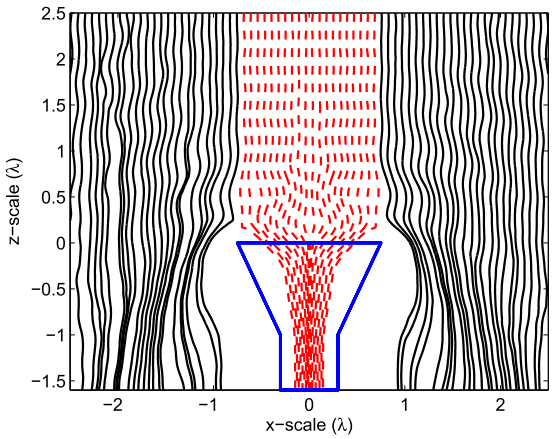

(b)

Fig. 4. Poynting streamlines for a tradition TE_{10}-mode rectangular horn antenna. The dimension of horn antenna is $0.75\lambda \times 1.5\lambda$ and the aperture efficiency is 0.8. (a) E-plane. (b) H-plane.

In Fig. 4, the terminated Poynting streamlines by the antenna load in the E-plane and H-plane are located within the antenna physical aperture size. In the 45° and 135° cut planes shown in Fig. 5, streamlines beyond the antenna physical area are absorbed by the load. This shows that for a nonsuperdirective aperture antenna, energy propagation outside the antenna physical area can be absorbed by the antenna load.

III. SUPERDIRECTIVE HORN ANTENNA DESIGN

We now consider the use of the Poynting streamline approach in guiding the design of superdirective aperture antennas. As observed earlier, one might conjecture that the Poynting streamline area shape should be circular to fully utilize the space around the antenna for an effective high-gain antenna. For the horn antenna in Fig. 5, there is a "notch" in the middle of the Poynting streamline area along the vertical direction that less efficiently utilizes the physical aperture of the horn antenna, while the area for dipole antenna is elongated in the vertical direction. Motivated by the Poynting streamline analysis, a screen can be placed in front of the horn antenna to achieve a more convex streamline area.

A design based on the Poynting streamline approach is shown in Fig. 6. Two rows of conducting rods are placed in the front of the horn antenna considered in Section II-B. The rods can be considered as a resonant parasitic dipole array. The induced current on the dipole array element can be controlled by changing the length of the

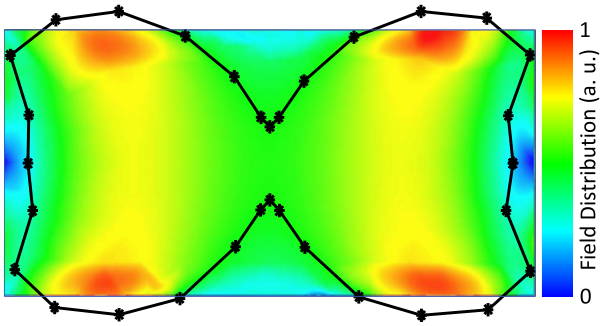

Fig. 5. Poynting streamline area shape for a TE_{10}-mode horn antenna with 0.8 aperture efficiency and the horn aperture field distribution corresponding to a normally incident plane wave.

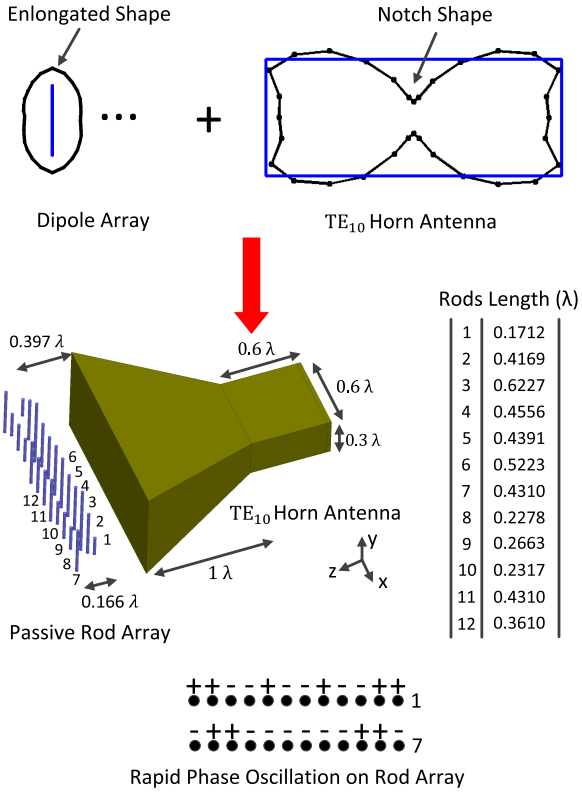

Fig. 6. Poynting streamline method is used to guide a superdirectivity antenna design. Two rows of symmetric passive dipole array are located in front of a traditional TE_{10} horn antenna. Enlongated Poynting streamline area for dipole array is used to compensate the notch shape in the Poynting streamline area for the horn antenna. Similar to a superdirective dipole array, the current distribution on the rods exhibits rapid phase oscillation. Aperture efficiencies for the TE_{10} horn antenna and superdirective horn antenna are 0.8 and 1.9, respectively.

rods. Superdirectivity can be implemented by optimizing the induced current on the rod elements. Similar to a superdirective dipole array, the current distribution on the rods exhibits a rapid phase oscillation. The rods in the second row are used to reduce the backscattered fields from the rods in the first row to the horn antenna and increase the forward radiation. The impedance match between the horn antenna and the antenna load improves with the added screen to an S_{11} of -19 dB at the design center frequency.

For the horn antenna with a 0.17λ thick screen, the radiating mode is broadside to the screen and the horn aperture, and the directivity is increased by enhancing the dimension of the screen and horn laterally rather than axially like Yagi–Uda antennas. There is a well-defined aperture and this particular antenna may be considered to be superdirective by the IEEE definition of the term. Based on this

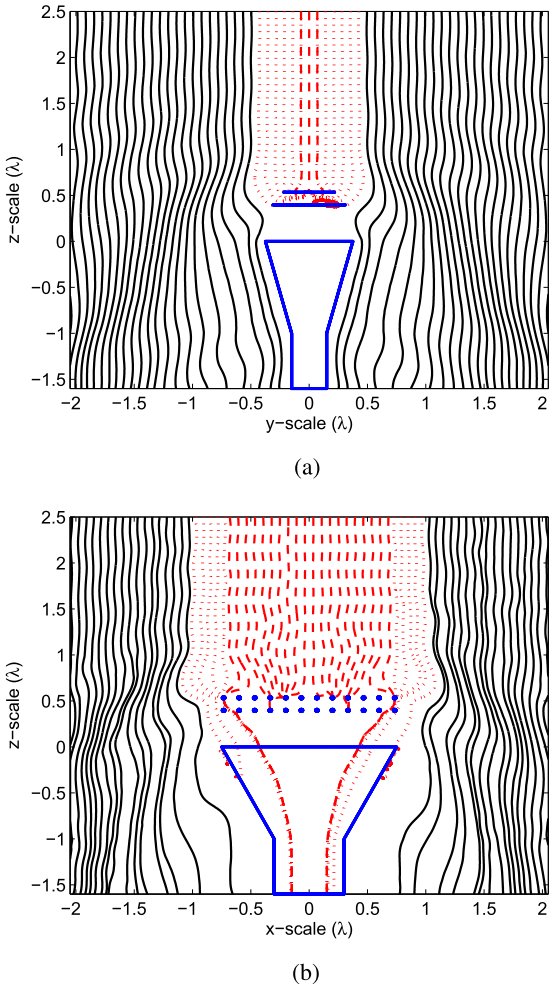

Fig. 7. Poynting streamlines for a superdirective horn antenna with 1.9 aperture efficiency. Dashed lines: streamlines terminated at the load of the bare horn antenna with 0.8 aperture efficiency. Dotted lines: additional Poynting streamlines terminated by the superdirective antenna load. (a) E-plane. (b) H-plane.

definition, the modeled aperture efficiency of the horn antenna with rods is 1.9, which is significantly higher than that of the bare horn antenna, for which the aperture efficiency is 0.8.

Fig. 7 shows the Poynting streamlines for the superdirective horn antenna in the E-plane and H-plane. Streamlines between the screen and the horn are not computed, because the streamlines become convoluted and cannot be extracted at the simulation resolution. Fig. 8 shows the effective area shapes for the traditional and superdirective horn antennas. The Poynting streamline area of the superdirective antenna is larger than the physical aperture area, which indicates that fields outside the antenna physical aperture area can be absorbed by the antenna load.

Most earlier investigations of superdirectivity have been confined to antenna arrays with rapid phase oscillations and electrically small antennas with strongly resonant structures [5], [11]–[13]. For aperture antennas, methods have been developed to enhance aperture efficiency, but most designs approach an efficiency of 100% and are not superdirective. The screened horn described here achieves a higher aperture efficiency than any other realistic design of which we are aware.

A. Overcoming Practical Limitations of Superdirective Antennas

A practical limitation for superdirective antennas is the narrow frequency bandwidth. If the operating frequency is offset from the design

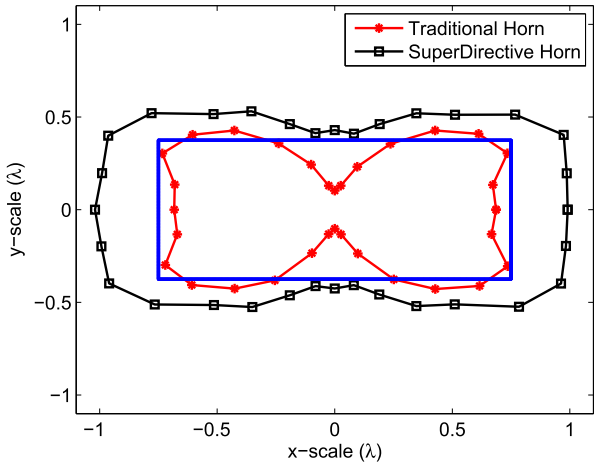

Fig. 8. Effective area shape calculated from streamlines captured by a traditional horn antenna and a superdirective antenna with the same physical size. Straight lines: physical size of the horn antenna aperture.

frequency, the superdirectivity is eliminated [5]. Superdirectivity is sensitive to the excitation currents on the rods, which depends on the length of the rod elements and the aperture field distribution of the horn antenna. When the frequency is changed, currents distributions on the rods are no longer tuned to attract Poynting streamlines.

Antenna efficiency and input reflection coefficient are shown over frequency for the superdirective horn antenna in Fig. 9. Antenna efficiency is the product of the aperture efficiency and radiation efficiency. The superdirectivity radiation bandwidth for the two-row rods horn design is 2.1%. A wider bandwidth superdirective antenna is designed by using only one row of resonant rods. As shown in Fig. 9, although the maximum aperture efficiency is decreased to 1.3, the superdirectivity radiation bandwidth increases to 8.4% and the impedance bandwidth becomes larger. Superdirectivity requires a high Q value and a strong resonance of the antenna, but by lowering the aperture efficiency target, the Q value decreases and the superdirectivity bandwidth becomes wider.

Besides narrow frequency bandwidth, low radiation efficiency is another practical limitation for the superdirective antennas due to ohmic or dielectric losses exacerbated by intense near fields and currents on the antenna structure. The ohmic loss of the two-row superdirective antenna is studied in Fig. 9(a). When the material of the rods is modeled as brass, the antenna efficiency of the superdirective antenna is decreased by 6% and the bandwidth of superdirective operation is increased by 33%. The increase of superdirectivity bandwidth is due to the lower Q value when the lossy material is used for the antenna. The simple structure of the rod screen, the use of metal only for the directivity-enhancing structure, and its location at the aperture rather than near the feed point help to minimize losses that would otherwise diminish the gain of the antenna.

Another practical limitation on superdirectivity is the extreme sensitivity of gain to fabrication errors [5]. For our design, the sensitivity to rod length is actually quite reasonable. The rod lengths can be increased by 1.4% and 11.5% for the two-row and one-row horns, respectively, before the aperture efficiency reduces to unity. This is well within the tolerance of standard manufacturing techniques.

B. Poynting Streamlines and Effective Area

We conjecture that the area of the locus of terminated Poynting streamlines is equal to the effective area calculated from the antenna directivity. We compare the Poynting streamline area A_s calculated from the shape area using the Poynting streamline method to the

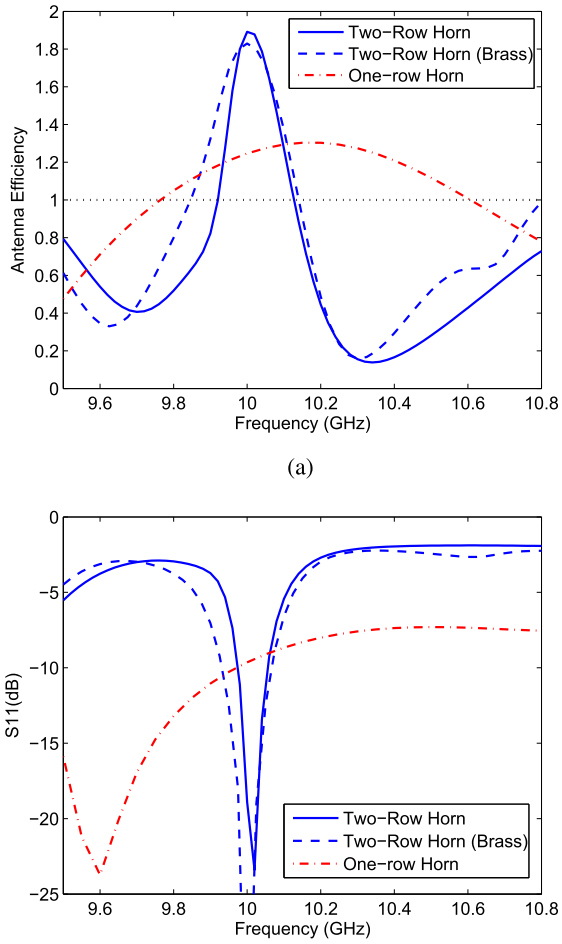

Fig. 9. Antenna efficiency and antenna S parameters for superdirective horn antennas over frequencies. One-row and two-row rod horns are used for the narrow and wide bandwidth design, respectively. The two-row screen with brass material quantifies the reduction in gain due to ohmic loss. (a) Antenna efficiency. (b) Antenna S parameters.

effective area calculated from $A_e = \lambda^2 D/(4\pi)$, where D represents the antenna directivity in Table I. The maximum difference is 6.6%. Numerical error in the field distribution, integrating the streamlines, and the cut plane approach limit the accuracy of the calculation, but this communication provides numerical evidence that the area of captured streamlines is equal to the effective area.

IV. Conclusion

Using the method of Poynting streamlines, we have studied linear, aperture, and superdirective receiving antennas. Using the locus of streamlines terminated by the antenna load, effective area shapes are given. Poynting streamline method is used to guide the high-directivity antenna design. A superdirective screened horn antenna with 1.9 aperture efficiency is compared with a traditional TE_{10}-mode horn antenna, which has an aperture efficiency of 0.8. To the best of our knowledge, no superdirective antenna with such large electrical aperture and high aperture efficiency exists. The narrow bandwidth characteristic of superdirective antennas is considered, and a superdirective antenna with 1.3 aperture efficiency is designed with a factor of four larger superdirectivity bandwidth and less manufacture error requirement than the antenna with 1.9 aperture efficiency. Unlike many previous superdirective array antennas, the screened horn does not suffer from low radiation efficiency.

We show numerically that the area of the locus of streamlines terminated by the antenna load is close to the effective area of the

antenna, and so we suggest this locus is similar to the effective area shape. The effective area shape might be considered as a supplementary to the IEEE standard definition of the effective area based on the strict mathematical demonstration. Proof that area of the locus of captured streamlines is equal to effective area remains an open question. The closed form solutions for the basic source, such as small electric and magnetic dipole, are instructive for the future work. There are also likely other types of antenna structures that could be enhanced using visualizations of the Poynting streamlines around the antenna.

ACKNOWLEDGMENT

The authors would like to thank Z. Yang for useful discussions on the physics of receiving antennas.

REFERENCES

[1] R. W. Sharpe, "Differential geometry," in *Graduate Texts in Mathematics*, New York, NY, USA: Springer, vol. 166. 1997.

[2] B. Müller, "Energy flow in the near field of a receiving antenna(electromagnetic near field energy flow characteristics of dipole/monopole receiving rod antenna, investigating frequency dependence of antenna effective area shape)," *Arch. Elektronik Uebertragungstechnik*, vol. 26, no. 10, pp. 443–449, Oct. 1972.

[3] G. Greving, "Gain calculation of thin wire antennas using the effective area approach and some inherent problems," *Arch. Elektronik Uebertragungstechnik*, vol. 32, pp. 49–56, Feb. 1978.

[4] E. Shamonina, V. A. Kalinin, K. H. Ringhofer, and L. Solymar, "Short dipole as a receiver: Effective aperture shapes and streamlines of the Poynting vector," *IEE Proc.-Microw., Antennas Propag.*, vol. 149, no. 3, pp. 153–159, Jun. 2002.

[5] R. C. Hansen, "Fundamental limitations in antennas," *Proc. IEEE*, vol. 69, no. 2, pp. 170–182, Feb. 1981.

[6] T. S. Bird and C. Granet, "Optimization of profiles of rectangular horns for high efficiency," *IEEE Trans. Antennas Propag.*, vol. 55, no. 9, pp. 2480–2488, Sep. 2007.

[7] R. J. Bauerle, R. Schrimpf, E. Gyorko, and J. Henderson, "The use of a dielectric lens to improve the efficiency of a dual-polarized quad-ridge horn from 5 to 15 GHz," *IEEE Trans. Antennas Propag.*, vol. 57, no. 6, pp. 1822–1825, Jun. 2009.

[8] H. F. Ma, X. Chen, H. S. Xu, X. M. Yang, W. X. Jiang, and T. J. Cui, "Experiments on high-performance beam-scanning antennas made of gradient-index metamaterials," *Appl. Phys. Lett.*, vol. 95, no. 9, p. 094107, 2009.

[9] E. A. Jones and W. T. Joines, "Design of Yagi–Uda antennas using genetic algorithms," *IEEE Trans. Antennas Propag.*, vol. 45, no. 9, pp. 1386–1392, Sep. 1997.

[10] *IEEE Standard Definitions of Terms for Antennas*, IEEE Standard 145-2013, 2013.

[11] L. J. Chu, "Physical limitations of omni-directional antennas," *J. Appl. Phys.*, vol. 19, no. 12, pp. 1163–1175, 1948.

[12] V. V. Veremey and R. Mittra, "Scattering from structures formed by resonant elements," *IEEE Trans. Antennas Propag.*, vol. 46, no. 4, pp. 494–501, Apr. 1998.

[13] A. E. Krasnok, D. S. Filonov, C. R. Simovski, Y. S. Kivshar, and P. A. Belov, "Experimental demonstration of superdirective dielectric antenna," *Appl. Phys. Lett.*, vol. 104, no. 13, p. 133502, 2014.